Inexpensive Room Temperature Ionic Liquids for Low Volatility Electrolytes of Dye-Sensitized Solar Cells

Shu-Yuan Ku and Shih-Yuan Lu[*]

Department of Chemical Engineering, National Tsing-Hua University, Hsinchu 30013, TAIWAN
[*]E-mail: sylu@mx.nthu.edu.tw

A quaternary ammonium salt based room temperature ionic liquid (RTIL) is developed to serve as the solvent and redox ion source for the preparation of low volatility electrolytes of dye sensitized solar cells (DSSCs). As compared with the conventional imidazolium-based RTILs for low volatility electrolytes, the present system possesses the advantages of cost effectiveness, easy preparation, and better environmental friendliness. For a specific case, acetylcholine iodide is mixed with ethylene glycol at a molar ratio of 1:9 to form an RTIL by heating the mixture at 70 $^{\circ}$C. This RTIL exhibits a loss rate of 0.0017 g h^{-1} at 70 $^{\circ}$C, showing its low volatility. The electrolyte prepared by dissolving 0.8M LiI, 0.1M I$_2$, and 0.5M N-methylbenzimidazole in the RTIL exhibits a viscosity of 24.5cp, an ionic conductivity of 5.47 mS cm^{-1}, and an ionic diffusion coefficient of 3.98x10^{-7} cm^2 s^{-1}. When applied to a DSSC that uses a metal-free indoline dye D-149 as the sensitizer, the above electrolyte gives a power conversion efficiency of 3.36%, 82% of that achieved by using the electrolyte prepared with the traditional organic solvent, acetonitrile, under the same measurement conditions.

1. INTRODUCTION

Dye sensitized solar cells (DSSC), because of their high efficiency to cost ratios, remain as one of the promising alternative clean energy harvesting technologies and continue to draw a great deal of research attention.[1] Electrolytes are one of the four key components of DSSCs, in addition to photoanodes, counter electrodes, and dyes, on which intensive and extensive research has been conducted [1-5]. Traditionally, electrolytes for DSSCs are prepared by dissolving redox ion sources in organic solvents, such as acetonitrile (AN), because of the low viscosity, high salt solubility, and good electrode wettability of organic solvents. These organic solvents are however often highly volatile and environmentally unfriendly. Particularly, their high volatilities lead to serious solvent evaporation

problems for the electrolytes and pose a great challenge to the practical application of DSSCs. Consequently, the development of electrolytes with low volatilities has drawn a great deal of research attention in recent years. Imidazolium salts, a class of room temperature ionic liquids (RTIL), possess extremely low volatilities and excellent ionic conductivities, and are thus considered a promising alternative to the commonly used organic solvents for electrolyte preparations [3,6-7]. In fact, these imidazolium salts serve not only as the solvent but also the redox ion source. Imidazolium salts however are expensive and environmentally concerned [8,9].

In this article, quaternary ammonium salt based RTILs are developed for preparations of low volatility electrolytes of DSSCs. This type of RTILs can be easily prepared by simply mixing and heating a quaternary ammonium salt with a hydrogen bond donor at a temperature often lower than 100°C. A wide variety of such RTILs may be produced since there is a large selection of quaternary ammonium salts and many hydrogen bond donors are available including amides, acids, alcohols, and amines [10]. In addition to easy preparation, this type of RTILs is also cost effective and environmentally friendly [9,10]. Jhong et al. made an attempt of using a quaternary ammonium salt based RTIL, choline iodide/glycerol (CI/G, molar ratio of CI:G=1:3 with 15 wt% water), as an ingredient in the formulation of a low volatility electrolyte for DSSCs [8]. They mixed CI/G with 1-propyl-3-methylimidazolium iodide (PMII), a popular imidazolium based RTIL, at a volume ratio of 7:13 as the solvent and redox ion source of the electrolyte and obtained a power conversion efficiency of 3.88%, 79% of that achieved by the DSSC using an electrolyte prepared from a mixture of two organic solvents, acetonitrile and valeronitrile at a volume ratio of 85:15. They successfully reduced the usage of imidazolium-based RTILs while maintaining a reasonable power conversion efficiency level. Nevertheless, the imidazolium salt, PMII, was still the main ingredient accounting for almost 2/3 of the electrolyte. The success of their work could have been contributed mainly by the imidazolium salt instead of the quaternary ammonium salt based RTIL, CI/G. An electrolyte system based on plain quaternary ammonium salts remains to be developed.

In this work, we develop low volatility electrolytes by using *plain* quaternary ammonium salt based RTILs as the solvent and redox ion source. Acetylcholine iodide (ACI) is used as the quaternary ammonium salt and ethylene glycol (EG) as the hydrogen bond donor to form RTILs, denoted as ACI/EG. The loss rate at heating and viscosity of this ionic liquid are measured, and electrolytes prepared based on it are characterized by ionic diffusion coefficients, viscosities, and ionic conductivities. Cell performances of the DSSCs assembled based on the prepared electrolytes are characterized. A power conversion efficiency of 3.36% is obtained, which is 82% of that achieved by the DSSC assembled using the electrolyte prepared by using acetonitrile as the solvent. This work demonstrates the success and promise of quaternary ammonium salt based RTILs for preparation of low volatility electrolytes for DSSCs.

2. EXPERIMENTAL

2.1. Preparation of ACI/EG and electrolytes

The room temperature ionic liquid ACI/EG is prepared by simply mixing ACI and EG at a desired molar ratio, followed by stirring and heating at 70 ^{o}C till a clear solution is obtained. The

corresponding electrolytes are prepared by dissolving suitable amounts of LiI, I_2, and N-methylbenzimidazole (NMBI) in ACI/EG to provide the I^-/I_3^- redox couple. For data reported here, the ACI:EG ratio is set at 1:9, the concentrations of I_2 and NMBI at 0.1 M and 0.5 M, respectively, and the concentration of LiI varying from 0.3 to 1.0 M. As for the comparison case, AN-based electrolyte, 0.5 M LiI, 0.05 M I_2, and 0.5 M 4-tert-butylpyridine (TBP) are dissolved in acetonitrile.

2.2. Cell assembly

The cell assembly follows the procedures of our previous work with necessary modifications [11]. Fluorine doped tin oxide (FTO) glass is used as the transparent conductive substrate. Commercial TiO_2 nanoparticles, P25, are cast onto the FTO glass with a doctor-blade technique to serve as the photoanode. The prepared photoanode is calcined in air at 450 ^{o}C for 30 min. Another TiO_2 layer, formed from commercial anatase TiO_2 particles of 300 nm, is cast on top of the photoanode to serve as the scattering layer. The thickness of the photoanode is controlled at around 8 μm, whereas the thickness of the scattering layer at around 5 μm. The $TiCl_4$ treatment is conducted by immersing the electrode in 0.2M ethanolic solution of $TiCl_4$ at 80 ^{o}C for 1 h, followed by calcination at 450 ^{o}C for 30 min. The $TiCl_4$-treated electrode is then immersed in a 0.3 mM metal-free organic dye solution, $C_{42}H_{35}N_3O_4S_3$ (D-149) in acetonitrile/t-butanol (volume ratio of 1:1), for 24 h, followed by rinsing in absolute ethanol to remove un-adsorbed dyes. Platinum of 100 nm thick is coated on a silicon wafer, pre-coated with a Cr layer of 30 nm thick, to serve as the counter electrode. The dye loaded photo-anode and Pt counter electrode are sealed together with a sealing material, SX 1170-25 from Solaronix, around the TiO_2 active area. The electrolyte is then introduced into the cell to complete the assembly.

2.3. Characterizations

The current density-voltage (J-V) curves of the cells are recorded with a potentiostat/galvanostat (CHI650B, CH Instruments, Inc.) under illumination of an Oriel Class A solar simulator (Oriel 91195A, Newport Corp.; AM 1.5, 100 mW cm^{-2}) calibrated with an Oriel reference Si solar cell (Oriel 91150, Newport Corp.). The monochromatic incident photon-to-current conversion efficiency (IPCE) is recorded by use of a monochromator (Oriel 74100, Newport Corp.) at the short circuit condition, with the intensity of each wavelength in the range of 1-3 mW cm^{-2}. The diffusion coefficient of the triiodide ion is derived from the limiting current density measured with the polarization experiment conducted at a symmetric thin cell composed of two Pt electrodes and the electrolyte to be tested [12]. The J-V curves are recorded at a scan rate of 10^{-2} V s^{-1} in a potential window of -1.0 to 1.0V to obtain the limiting current density.

3. RESULTS AND DISCUSSION

The volatility of ACI/EG is first characterized to prove its low volatility by directly heating the sample at 70 ^{o}C in an oven to measure the apparent mass loss rate. Figure 1 shows the mass loss curves

of ACI/EG and acetonitrile. Evidently, the mass of acetonitrile drops to zero quickly, whereas that of ACI/EG exhibits a slow decreasing trend over a long period of 650 h. The apparent mass loss rate of ACI/EG as determined from Fig. 1 is 0.0017 g h^{-1}, two orders of magnitude smaller than 0.45g h^{-1} of acetonitrile, showing the low volatility of ACI/EG. The formation of hydrogen bonds between the iodide of ACI and the proton of the hydroxyl groups of EG may be inferred from a comparison of the FTIR spectra recorded for EG and ACI/EG, as shown in Fig. 2.
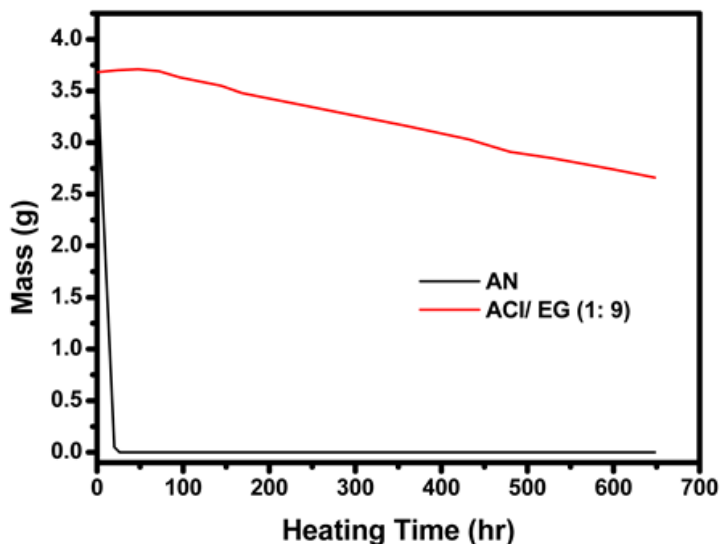

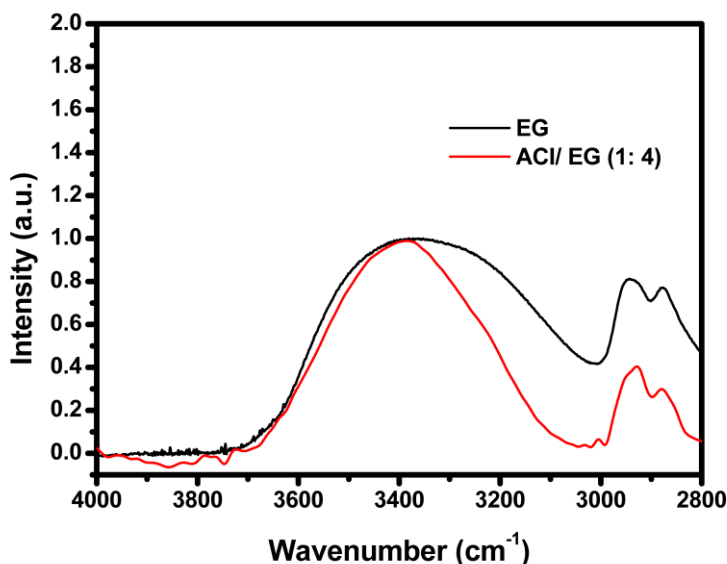**Figure 1.** Mass loss curves of ACI/EG and acetonitrile.

Figure 2. FTIR spectra of ACI/EG (1:4) and EG.

The two absorption peaks located in the region of 2800-3000 cm^{-1} are contributed by the C-H stretching, whereas the broad peak centering around 3400 cm^{-1} comes from the O-H stretching.

Evidently, the stretching peak of O-H becomes narrower toward the higher wavenumber region for the ACI/EG sample. This phenomenon implies a more restricted bond stretching caused by the hydrogen bond formation between ACI and EG [13].

There are two important functionalities for a good electrolyte of DSSCs to perform, one is to regenerate the dye molecules by oxidizing I^- to form I_3^- and the other is to transport I_3^- from the photoanode to the counter electrode to receive electrons there to regenerate I^- and continue the redox cycle. It is essential to regenerate the dye molecules and I^- timely so that the electrons injected by the excited dye molecules to the conduction band of the titania photoanode would not combine with the oxidized dye molecules or I_3^-, occurrence of which leads to reduction in collected electrons for external loads, i.e., lowering of the power conversion efficiency. To this end, the concentration of I^- and transport properties of I_3^- are important parameters for the electrolytes. We investigate the performances of the ACI/EG-based electrolytes and the subsequently assembled DSSCs as functions of the concentration of LiI. Key performance indices, including the apparent I_3^- diffusion coefficients (D), viscosities (μ), and ionic conductivities (κ) of the electrolytes, and the short-circuit current densities (J_{sc}), open-circuit voltage (V_{oc}), fill factor (FF), power conversion efficiencies (η), maximum quantum efficiencies of the incident photon-to-current conversion efficiency (IPCE) spectra (MQE), and Nernst diffusion resistances (R_D) of the corresponding DSSCs, are tabulated in Table I. Also included in Table I are data obtained for the AN-based electrolyte and corresponding DSSC for comparison.

Table 1. Characteristics of electrolytes and DSSCs based on them as functions of LiI concentration in electrolytes, including apparent I_3^- diffusion coefficients (D), viscosities (μ), ionic conductivities (κ), short-circuit current densities (J_{sc}), open-circuit voltage (V_{oc}), fill factor (FF), power conversion efficiencies (η), maximum quantum efficiencies of IPCE spectra (MQE), and Nernst diffusion resistance (R_D). Also included are data obtained for AN-based electrolyte for comparisons.

LiI, [M]	$D*10^{7}$,[a] [$cm^2 s^{-1}$]	μ,[b] [cp]	κ,[c] [$mS\ cm^{-1}$]	J_{sc}, [$mA\ cm^{-2}$]	V_{oc}, [V]	FF [-]	η, [%]	MQE [%]	R_D, [Ω]
0.3	2.87	19.8	4.61	6.93	0.68	0.62	2.9	31.9	13.5
0.5	3.76	21.9	5.02	7.52	0.67	0.62	3.1	41.2	7.8
0.8	3.98	24.5	5.47	8.57	0.645	0.61	3.36	48.2	6.9
1.0	3.71	27.8	5.22	6.53	0.6	0.59	2.3	35.4	7
AN	36.7	1.1	9.94	10.24	0.67	0.59	4.1	49.2	0.7

[a] determined from limiting current density obtained with polarization measurements of thin layer cells [13]
[b] measured with a rotational viscometer (DV-III Rheometer, Brookfield)
[c] measured with a conductivity meter (C-561, Consort)

The increase in LiI concentration produces two opposite effects on D and κ. Higher concentrations of LiI lead to higher concentrations of I^- and I_3^-. Here, I_3^- comes from the reaction of I^- with I_2. This is beneficial for both the I_3^- diffusion and overall ionic conductivity. On the other hand,

the electrolyte viscosity increases with increasing concentration of LiI, resulting in higher transport resistances to ionic species and thus an opposite effect on D and κ. As a result of the competition of the two opposite effects, D and κ reach their maxima at an optimal LiI concentration, 0.8M for the present system. Another factor may have also contributed to the occurrence of the maximum D and κ with increasing concentration of LiI. According to the pair-ion model proposed by Robinson and Stokes,[14] the structure of the ionic species in solution may change from the solvation ion mode to contact ion mode when the concentration of the ionic species exceeds some critical value. The formation of contact ions reduces the ionic mobility and thus the diffusion coefficient and ionic conductivity. As a result, maximum values of D and κ are reached with increasing concentration of LiI for the present electrolytes. As evident from Table I, although the values of D and μ of the ACI/EG-based electrolytes are one order of magnitude lower and higher, respectively than those of the AN-based electrolyte, the values of κ of both systems are comparable. This is probably because of the extra ionic species provided by ACI/EG. Note here ACI/EG serves not only as a solvent, but also a redox ion source. This is also one advantage of using RTILs as the solvent for DSSCs.
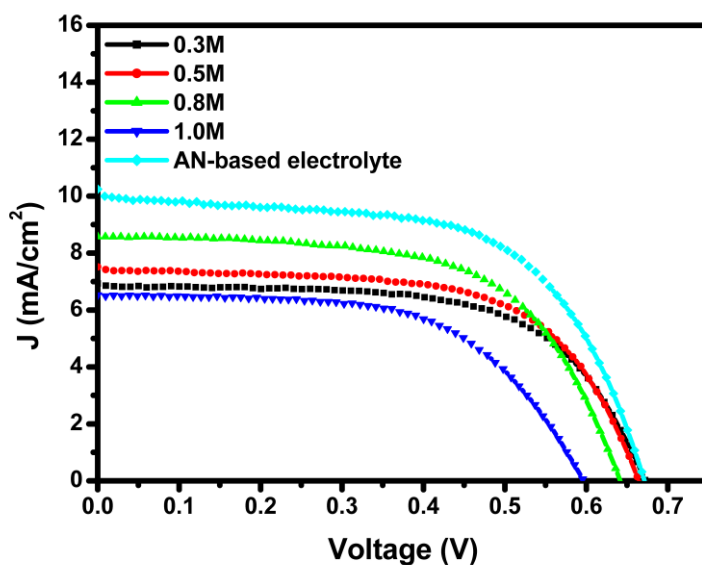

Figure 3. J-V curves for DSSCs assembled from using ACI/EG-based electrolytes (ACI/EG of 1:9 molar ratio+0.1M I_2+0.5M NMBI+xM LiI) at four different concentrations of LiI. Also included is J-V curve for the DSSC using AN-based electrolyte.

Figure 3 shows the J-V curves of five DSSCs assembled based on five different electrolytes: ACI/EG-based with an LiI concentration of 0.3, 0.5, 0.8, or 1.0M and one AN-based. As expected, the AN-based DSSC performs the best, with higher current densities and a wider operation voltage widow. For ACI/EG-based DSSCs, both V_{oc} and FF decrease with increasing LiI, whereas a maximum is reached for J_{sc}, the same trend as for D and κ. As the concentration of LiI increases, the concentration of I^- increases, giving faster dye regeneration for further photon-induced electron generation and injection, and thus an increase in J_{sc}. Nevertheless, too high of an LiI concentration gives an excess

amount of I_3^- and increases the combination probability between the conduction band electrons of the titania photoanode and I_3^-, resulting in a decrease in J_{sc}. If examined closely, the variations in J_{sc} are more significant than those in V_{oc} and FF, and dominate the results of η. Note that the variation ranges are only 13% for V_{oc} and 5% for FF, but 31% for J_{sc}; and the power conversion efficiency is directly proportional to the product of V_{oc}, FF, and J_{sc}. Consequently, a maximum power conversion efficiency of 3.36% is obtained at the LiI concentration of 0.8M. This value is 82% of that achieved by the AN-based DSSC. The power conversion efficiencies obtained in this work are significantly lower than those reported in the literature mainly because of the use of the metal-free organic dye D-149. In the past decade, there have been a great deal of research attention paid to develop metal-free organic dyes in an attempt to reduce the dye cost by removing the expensive and rare metals, such as Ru, from the dye molecules [15]. There are however still a lot of room for improvement for organic dyes in terms of efficiency. We use the much cheaper organic dye to go with the cost effectiveness theme of the present work.

Figure 4 shows the IPCE spectra of the five DSSCs. IPCE measures how effective incident photons can be converted into collected electrons for the external loads at different wavelengths. The resulting trend follows that for the power conversion efficiency, with the AN-based DSSC outperforming the ACI/EG-based DSSCs over the entire wavelength range. Among the ACI/EG-based DSSCs, the one containing 0.8M LiI gives the best efficiencies. The maximum efficiency of each IPCE spectrum is included in Table I for comparison.
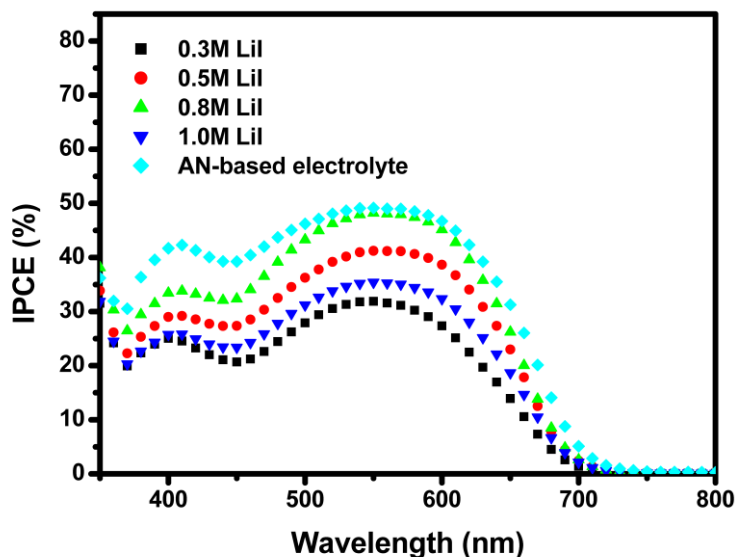

Figure 4. IPCE spectra for DSSCs assembled from using ACI/EG based electrolytes (ACI/EG of 1:9 molar ratio+0.1M I_2+0.5M NMBI+xM LiI) at four different concentrations of LiI. Also included is IPCE spectrum for the DSSC using AN-based electrolyte.

We further conduct the electrochemical impedance spectroscopy on all five DSSCs, from which the impedances to charge transport occurring at the different parts of the cell can be investigated

for cell performance analyses. Fig. 5 shows the Nyquist plot of two DSSCs, one ACI/EG-based and the other AN-based, for comparison. For a typical DSSC, the impedances existing in the system can be divided into four parts in series, including the resistances presented by the electrodes and external circuit (R_s), the charge transfer impedance occurring at the counter electrode/electrolyte interface (R_{CE}), the Nernst diffusion resistance for the electrolyte (R_D), and the charge transfer impedance accounting for the electron diffusion across the titania layer and the back electron transfer reaction with the oxidized state of the redox couple of the electrolyte at the titania/electrolyte interface (R_{TiO2}) [16]. A typical Nyquist plot for a DSSC shows two to three arcs, with the first arc, corresponding to the high frequency region and representing R_{CE}, intercepting the horizontal axis at R_s. The second arc is contributed by R_{TiO2} and appears at the intermediate frequency region. The third arc, corresponding to the low frequency region and representing R_D, is often too small to be observed for DSSCs assembled by using organic solvent based electrolytes. From the figure, evidently, the third arc for the AN-based DSSC cannot be clearly identified in the plot, indicating the small electrolyte diffusion resistance. As for the ACI/EG-based DSSC, all three arcs can be identified and the third arc is clearly shown, implying an appreciable diffusion resistance for the ACI/EG-based electrolyte. In the last column of Table I, we collect the fitted R_D values of the five DSSCs for comparison. Evidently, the AN-based DSSC possesses the lowest R_D, one order of magnitude lower than those of the ACI/EG-based DSSCs. Among the ACI/EG-based DSSCs, the one containing 0.8M LiI gives the lowest R_D, consistent with the relevant results of D and κ.
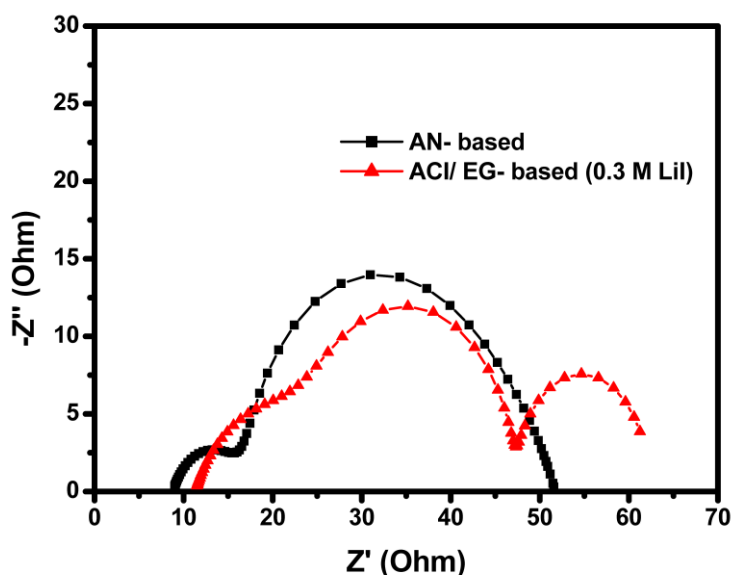

Figure 5. Nyquist plot for an ACI/EG-based (0.3M LiI) and an AN-based DSSCs.

4. CONCLUSION

A quaternary ammonium salt based room temperature ionic liquid, ACI/EG, is demonstrated to produce electrolytes with good functional properties. This type of RTILs has the advantages of cost

effectiveness, easy preparation, and better environmental friendliness, over the imidazolium-based RTILs as the low volatility alternative to the conventional organic solvents for electrolyte preparation. The ACI/EG-based DSSC shows a power conversion efficiency of 3.36%, 82% of that achieved by an AN-based DSSC. This demonstrates the success and promise of the present RTIL as a viable candidate for preparation of low volatility electrolytes for DSSCs, and the results of the present work are expected to foster further investigations in this area.

References

1. M. Gratzel, *Acc. Chem. Res.*, 42 (2009) 1788
2. J.-H. Yum, D.P. Hagberg, S.-J. Moon, K.M. Karlsson, T. Marinado, L. Sun, A. Hagfeldt, M.K. Nazeeruddin and M. Gratzel, *Angew. Chem. Int. Ed.*, 48 (2009) 1576
3. Y. Bai, Y. Cao, J. Zhang, M. Wang, R. Li, P. Wang, S.M. Zakeeruddin and M. Gratzel, *Nature Mater.*, 7 (2008) 626
4. C.-Y. Kuo and S.-Y. Lu, *Nanotechnology*, 19 (2008) 095705
5. C.-T. Hsiao, S.-Y. Lu and T.-Y. Tsai, *Chem. Europ. J.*, 13 (2011) 1358
6. D. Kuang, P. Wang, S. Ito, S.M. Zakeeruddin and M. Gratzel, *J. Am. Chem. Soc.*, 128 (2006) 7732
7. M. Wang, X. Xiao, X. Zhou, X. Li and Y. Lin, *Sol. Energy Mater. Sol. Cells.*, 91 (2007) 785
8. H.-R. Jhong, D. S.-H. Wong, C.-C. Wan, Y.-Y. Wang and T.-C. Wei, *Electrochem. Comm.*, 11 (2008) 209
9. A.P. Abbott, D. Boothby, G. Capper, D.L. Davies and R.K. Rasheed, *J. Am. Chem. Soc.*, 126 (2004) 9142
10. A.P. Abbott, P.M. Cullis, M.J. Gibson, R.C. Harris and E. Raven, *Green Chem.*, 9 (2009) 868
11. T.-Y. Tsai and S.-Y. Lu, *Electrochem. Comm.*, 11 (2009) 2180
12. M. Zistler, P. Wachter, P. Wasserscheid, D. Gerhard, A. Hinsch, R. Sastrawan and H.J. Gores, *Electrochim. Acta*, 52 (2006) 161
13. T. Zhou and J. Zhao, *J. Colloid & Interface Sci.*, 331 (2009) 476
14. R.A. Robinson and R.H. Stokes, *Electrolyte Solutions*, Butterworths, London (1959)
15. H. Imahori, T. Umeyama and S. Ito, *Acc. Chem. Res.*, 42 (2009) 1809
16. 1M. Adachi, M. Sakamoto, J. Jiu, Y. Ogata and S. Isoda, *J. Phys. Chem. B*, 110 (2006) 13872